Applied Energy 164 (2016) 294–302

Contents lists available at ScienceDirect

Applied Energy

journal homepage: www.elsevier.com/locate/apenergy

Comprehensive energy analysis of a photovoltaic thermal water electrolyzer

Muhammed E. Oruc [a], Amit V. Desai [a], Paul J.A. Kenis [a,*], Ralph G. Nuzzo [b,*]

[a] Department of Chemical and Biomolecular Engineering, University of Illinois, Urbana, IL 61801, United States
[b] Department of Chemistry, University of Illinois, Urbana, IL 61801, United States

HIGHLIGHTS

- A Photovoltaic Thermal Water Electrolyzer (PVTE) configuration is reported.
- The PVTE system was modeled to determine optimal geometry and operating conditions.
- The overall efficiency increased with the velocity of heat-transfer fluid.
- The max improvement in power output for the PVTE compared to a PV alone is in the afternoon.
- A PVTE (instead of a standalone electrolyzer) exhibits 2.5 times more hydrogen production.

GRAPHICAL ABSTRACT

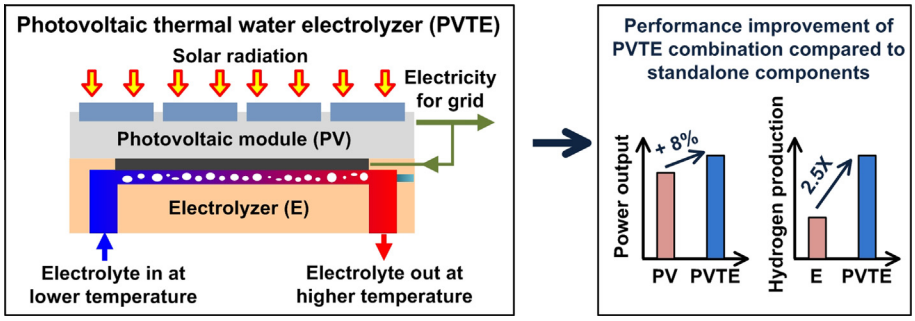

ARTICLE INFO

Article history:
Received 23 March 2015
Received in revised form 5 November 2015
Accepted 30 November 2015
Available online 22 December 2015

Keywords:
High-temperature electrolysis
COMSOL multiphysics
Artificial photosynthesis
Photovoltaic/thermal (PVT) system

ABSTRACT

The use of photovoltaic thermal (PVT) technologies enables improvement in the electrical efficiency of a photovoltaic (PV) module by reducing the temperature of the PV module via active waste heat removal. In current PVT systems, the removed heat is mainly used for specific applications, such as water and/or room heating, but their need is intermittent and seasonal. For a more efficient and versatile use of the removed waste heat, we propose a new architecture where the PV module is integrated with a dual-functional electrolyzer that removes the waste heat by active cooling and produces hydrogen via electrolysis. The excess heat from the PV cell is utilized to enhance the reaction kinetics of the electrolysis process (due to an increase in temperature) inside an electrolyzer, which is located below the PV module. In this paper, we used finite-element analysis (FEA) simulations to optimize the geometry and operating conditions of an electrolyzer to maximize overall energetic efficiency and hydrogen production. To evaluate the practical feasibility of the approach, we performed a comprehensive energy analysis of the PVTE system using data from Phoenix, AZ. The energetic efficiency of the proposed PVTE system was calculated to be 56–59%, which is comparable to those of current PVT systems. Additionally, the integration of the electrolyzer with the PV module led to an almost 2.5-fold increase in hydrogen production compared to a stand-alone electrolyzer operated at ambient temperature. The analyzed hybrid approach potentially represents a viable and useful alternative for utilization of waste heat energy from PV cells. This approach may further increase the use of photovoltaic technologies as a renewable energy source.

* Corresponding authors at: 600 South Mathews Avenue, Urbana, IL 61801, United States. Tel.: +1 (217) 244 9214 (P.J.A. Kenis), +1 (217) 244 0809 (R.G. Nuzzo).
E-mail addresses: kenis@illinois.edu (P.J.A. Kenis), r-nuzzo@illinois.edu (R.G. Nuzzo).

http://dx.doi.org/10.1016/j.apenergy.2015.11.078
0306-2619/

1. Introduction

Photovoltaic (PV) technologies employ the photovoltaic effect to convert solar energy into electricity. PV technologies are rapidly becoming an important component of the energy landscape. In fact PV is the third most important renewable energy source in terms of globally installed capacity [1]. To further exploit the potential of PV technologies, the energy output of these technologies needs to be increased. Several strategies have been employed to enhance the electrical conversion efficiency of PV cells, *e.g.*, by the use of new materials [2,3] and through development of sophisticated designs [4,5]. Despite these efforts, the electrical conversion efficiency, the fraction of incoming solar radiation that is converted to electricity, of PV cells currently on the market is still less than 20% [6]. Another strategy to improve the electrical conversion efficiency is to reduce the temperature of the PV cell, as the efficiency is known to decrease at higher temperatures [7]. This rise in temperature mainly originates from the energy that is not converted into electricity and dissipated as heat. Hence, active and passive cooling methods have been employed to remove waste heat, hereby increasing efficiency, and consequently energy output [8].

One approach to further increase the overall energy utilization of PV technologies is to convert the energy removed as waste heat into another useful form of energy, *e.g.*, use of hybrid photovoltaic/thermal (PVT) systems [9]. A PVT system combines a PV module that converts the solar energy into electricity, and a solar thermal collector module that absorbs some of the waste heat for later use (thereby also reducing the temperature of the PV module) [10,11]. The overall energetic efficiency (fraction of incoming solar radiation that is converted to electricity and useful heat energy) of PVT systems ranges from 53% to 68% based on the location and time [12]. Along with the advantage of a high overall energy efficiency, PVT systems also produce more energy per unit surface area [13] and reduce space and installation cost compared to a separate PV panel and a solar heat collector system.

In PVT systems the captured heat energy is typically used for domestic hot water and/or room heating. The need for these applications, however, is intermittent and seasonal, leading to stored energy being wasted. For instance, the overall energy output of PVT systems will be higher when the ambient temperature is high (due to higher level of solar radiation), but the need for hot water and heating during these times will be lower. As a result, a need exists for alternative ways to store and use the waste heat of PVT systems, especially ways that are less subject to intermittency and seasonal requirements. *To this end, we propose an integrated system – "a photovoltaic thermal water electrolyzer (PVTE)" – which comprises a PV cell positioned on top of a planar micro-water electrolyzer*. This system not only produces the same output as typical PVT systems, *i.e.*, electricity and heat energy, but also produces hydrogen, an environmentally benign and a sustainable energy carrier that can be stored and used for applications such as power generation when solar power is not available or transportation [14]. Naturally, hydrogen storage (*e.g.*, by compression) would require additional energy, but that energy cost is not included in the analyses reported here.

Fig. 1(a) provides a schematic illustration of the PVTE system, while the design and operation of the electrolyzer is illustrated in Fig. 1(b). Part of the electrical energy generated by the PV cell is used for water electrolysis, which is a promising approach for hydrogen production, while the remaining electrical energy is supplied to the grid, similar to conventional PVT systems [6,9]. The excess heat dissipated from the PV cell is captured by the water electrolyzer, which functions as a heat sink, and causes the temperature of the electrolyte in the electrolyzer to increase and approach the temperature of the PV cell. The higher temperature of the electrolyte in the electrolyzer increases the efficiency of the electrolysis reaction and also reduces the over-potentials for H_2 and O_2 gas evolution at the electrodes [15]. As a result, the dissipated heat energy is utilized to not only produce hydrogen, but also increase the efficiency of the electrolysis. Additionally, the electrolyte in electrolyzer functions as a heat-transport fluid, and the electrolyte at the elevated temperature (exiting the electrolyzer) is circulated to transfer heat to an insulated water tank, similar to the scheme used for domestic hot water and/or room heating in conventional PVT systems. The produced hydrogen can be used, for example, to operate a fuel cell for power generation, or as a fuel for a fuel cell-based car.

In this paper, we present a comprehensive analysis of the overall efficiency of the proposed PVTE configuration, and compare its performance to that of the PV panel alone. We also estimated the efficiency of the electrolysis process within the PVTE system and compared it to that of a stand-alone electrolyzer. COMSOL Multiphysics® software was used to predict the temperatures of the electrolyte and the PV cell for various values of ambient temperature and solar flux. We also used the simulations to optimize the chamber thickness of the electrolyzer and the flow velocity of the electrolyte with the objective of maximizing the electrical efficiency, thermal efficiency, and the efficiency of water electrolysis. To demonstrate the practical feasibility of the PVTE system, we estimated the hourly and monthly efficiency values of the various processes and the power output using solar irradiation and temperature data for Phoenix, Arizona from the year 2010. The high temperatures in combination with the abundant availability of solar power in Phoenix make this location an attractive location for employing a PVTE.

2. Computational model of PVTE

2.1. Dimension and material properties

In this work, we analyze a unit PV cell (16 cm × 16 cm) with 16 water electrolyzers underneath it. An illustration of the module with the various layers and thicknesses are shown in Fig. 2(a). The PV cell size was chosen such that the cell can be fabricated on a 6 in. silicon wafer. The solar cell portion of this module is sandwiched between two layers of ethylene vinyl-acetate (EVA) covered on top with a protective glass layer and on the bottom with a backing layer (Tedlar) to separate the cell from the electrolyzer. The different materials and the thicknesses of each of these protective layers were chosen based on prior reports on PVT systems [16,17]. The electrolyzer unit cell is 40 mm long, 40 mm wide, and ~9 mm thick, while the size of the electrolyzer chamber is 20 mm × 20 mm × 0.4 mm (Fig. 2(b)). These values for the electrolyzer dimensions were chosen to be compatible with the standard microfabrication procedures. Two 1 cm^2 thin-film electrodes are located in the chamber and on a non-electrically conductive glass substrate that is 1 mm thick. A 7 mm thick PDMS slab was chosen as the electrolyzer chamber material due to its low thermal conductivity. Our simulations indicated that the temperature of the PV cell did not change significantly for PDMS slabs with thickness exceeding 7 mm. The PDMS reservoir includes an inlet for the electrolyte at ambient temperature, and two outlets for the heated electrolyte, as well as the formed H_2 and O_2 gases. Properties of each material used in the COMSOL simulation are listed in Table 1.

2.2. Modeling of the heat transfer processes

To characterize the performance of the PVTE module, we used COMSOL Multiphysics® software to perform finite element analysis

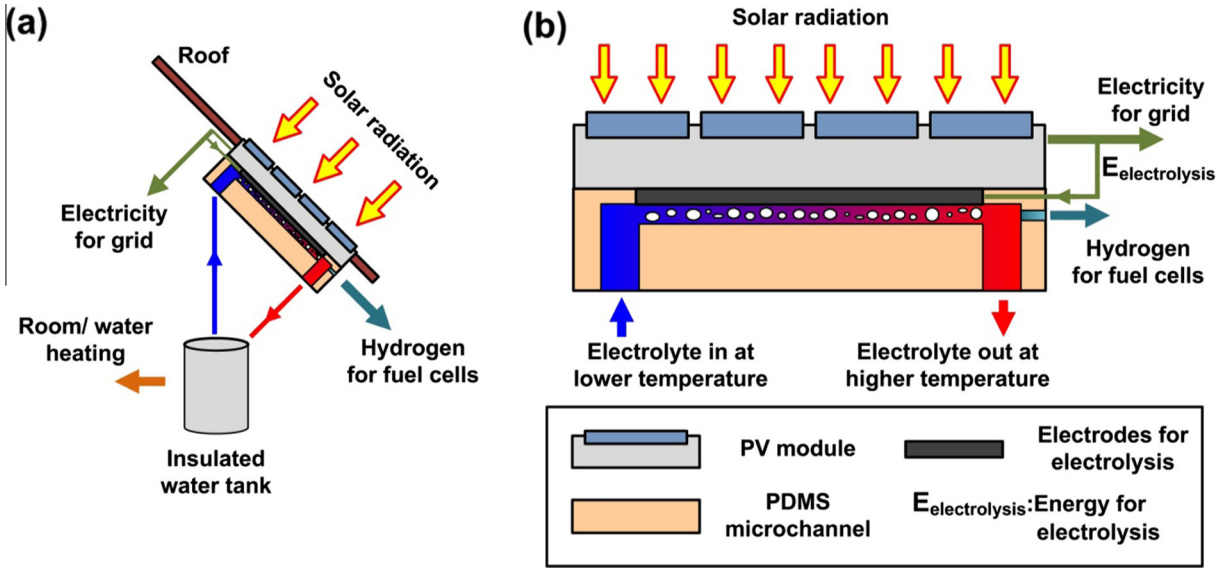

Fig. 1. Schematic illustration of (a) the overall PVTE system and (b) the design and operation of the electrolyzer. For clarity purposes, all the layers of the PVTE system are not shown and the components are not to scale.

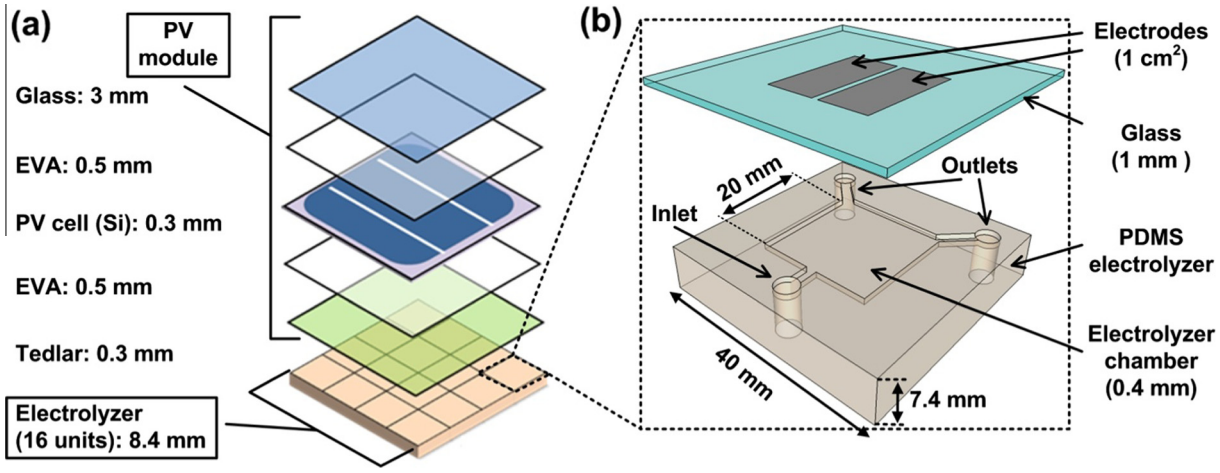

Fig. 2. (a) Illustration of the layered assembly of the PVTE system comprised of a PV module on top of an electrolyzer. (b) Magnified view of one electrolyzer unit cell with the electrodes patterned on glass.

Table 1
Properties of each material used in COMSOL simulation [16,17].

Layer/material	Density (kg/m^3)	Specific heat (J/kg/K)	Thermal conductivity (W/m/K)
Glass	2203	703	1.38
EVA	950	3135	0.23
PV cells (Si)	2330	700	130
Tedlar	1200	1090	0.16
PDMS	970	1460	0.15

(FEA) simulations. We first estimated the temperature of the PV cell, and the electrolyte temperature within and at the outlet of the electrolyzer for ambient temperature and a fixed value of solar flux. We systematically studied the effect of the chamber thickness of the electrolyzer and velocity of the electrolyte (coolant) on these temperatures. In the COMSOL simulations, all forms of heat transfer were considered. The analysis was performed for a unit cell and the cell was assumed to be infinitely long on each side and completely insulated. The absorbed heat due to the solar radiation was assumed to be transported from the PV cell to the electrolyzer via conduction. Heat dissipation to the surrounding was assumed to occur by convection and thermal radiation.

The solar energy that is irradiated on to the PV cell is reflected, absorbed, or transmitted. The absorption factor (A), the ratio of the absorbed energy to incident solar irradiance, of the PV cell for both crystalline silicon and thin-film solar cells plays an important role in the thermal efficiency of PVT collector systems. The absorbed solar energy that is not converted into electricity is transformed into heat. The fraction of incident solar irradiance that is converted into heat is called the effective absorption factor, which is given by

$$A_{eff} = A - \eta_e \quad (1)$$

where η_e is the electrical efficiency of the PV cell [18]. Typical values for absorption factors and effective absorption factors can vary between 70–90% and 60–80%, respectively [18]. For the simulations, A was assumed to be 90% (highest value reported in the literature) and η_e to be 15% (typical efficiency of PV cells). At steady state, the general heat conduction through the module is given by

$$\nabla \cdot (k\nabla T) = 0 \quad (2)$$

The heat loss by convection from the various surfaces of the module to the environment is given by

$$q_{conv} = -h_c \cdot A \cdot (T_{surface} - T_{amb}) \quad (3)$$

The average wind speed was assumed to be 1 m/s, which means that the heat transfer coefficient h_c is 6.5 W/m^2/K [17]. The heat loss by thermal radiation from the PV surface is given by

$$q_{rad} = \epsilon \cdot \sigma \cdot (T^4_{surface} - T^4_{amb}) \quad (4)$$

The average surface emissivity of silicon ϵ was assumed to be 0.85 and the Stefan–Boltzmann constant σ is 5.67×10^{-8} W/m^2/K^4 [18].

The conjugate heat transfer module in COMSOL allows analysis of the phenomenon of forced convection between the electrolyte as a heat carrier fluid and the high-temperature solar cell as a heat source. The forced convection is described using the continuity and momentum equations, and the heat transfer equation for the electrolyte as follows:

$$\nabla \cdot (\rho u) = 0 \quad (5)$$

$$\rho u \cdot \nabla u = \nabla p + \nabla \cdot (\mu(\nabla u + (\nabla u)^T)) \quad (6)$$

$$pC_p u \cdot \nabla T = \nabla \cdot (k\nabla T) \quad (7)$$

The initial temperature of the electrolyte was assumed to be equal to the ambient temperature [19]. The flow through the electrolyzer was assumed to be laminar and incompressible (based on the flow rates and fluid properties).

2.3. Evaluation of overall performance

2.3.1. Electrical efficiency of the PV Module

The operating temperature of the PV cell influences its electrical efficiency. Many parameters affect the temperature of the PV panels, including the ambient temperature, the local wind speed, the solar radiation flux, material properties, and the design of the PV system. Different equations and correlation coefficients have been proposed to estimate the electrical efficiency of the PV module as a function of its temperature [20,21]. In this work we use the equation below:

$$\eta_{PV} = \eta_{PV(ref)}[1 - \beta_{ref}(T - T_{ref})] \quad (8)$$

where $\eta_{PV(ref)}$ is the module's electrical efficiency at the reference temperature (with a value of 0.15), β_{ref} is the temperature coefficient (0.0041), and T_{ref} is the reference temperature (25 °C) [20].

2.3.2. Energetic and exergetic efficiency of the PVTE module

An important parameter used to characterize the performance of PVT systems is thermal efficiency ($\eta_{thermal}$), which is based on the first law of thermodynamics, and is given by [19,22]:

$$\eta_{thermal} = \frac{E_T}{E} \quad (9)$$

$$E_T = m_{electrolyte} * C_{electrolyte} * \Delta T_{electrolyte} \quad (10)$$

where E_T is the thermal output power, E is the irradiation per unit area, $m_{electrolyte}$ is the mass of the electrolyte, $C_{electrolyte}$ is the specific heat of the electrolyte, and $\Delta T_{electrolyte}$ is the temperature difference of the electrolyte entering and leaving the system.

The first law for thermodynamics can be used to estimate the amount of energy contained in the system, but not the amount of work performed on the external world (outside the system). A temperature difference between the heat source and the heat sink is necessary in order to extract energy as useful work, captured by the second law of thermodynamics. This useful work is also called exergy or available energy. The exergetic efficiency of system is given by [23]:

$$\varepsilon_{thermal} = \left(1 - \frac{T_{amb}}{T_{out}}\right) * \eta_{thermal} \quad (11)$$

where T_{amb} is the ambient temperature and T_{out} is the temperature of the electrolyte leaving the electrolyzer. The equation to calculate the exergetic output power, $\dot{E}x_t$, is given as below [23]:

$$\dot{E}x_t = \dot{E}_t\left(1 - \frac{T_{amb}}{T_{out}}\right) \quad (12)$$

where $\dot{E}_t$ is the thermal output power.

The expressions for overall energetic (1st law) and overall exergetic (2nd law) efficiencies of PVT systems are listed below, respectively

$$\eta_{PVT} = \eta_{PV} + \eta_{thermal} \quad (13)$$

$$\varepsilon_{PVT} = \varepsilon_{PV} + \varepsilon_{thermal} \quad (14)$$

where ε_{PV} is assumed to be equivalent to η_{PV} [23]. We used these equations to calculate energetic and exergetic efficiencies in case of our proposed PVTE system to be consistent with the terminology in the literature.

On the other hand, the final temperature of the water in the heat storage tank can be calculated simply from the equation below [23]

$$M_t C_t \frac{dT_t}{dt} = (\#\text{ of unit cell}) m_{electrolyte} C_{electrolyte}(T_{ti} - T_{to}) + (h_t A_t)(T_{amb} - T_t) \quad (15)$$

where M_t, C_t, T_t and A_t are respectively the lumped mass, the weighed-average specific heat capacity, temperature and the outside surface area of the water tank; T_{ti} and T_{to} are the electrolyte temperatures at the inlet and outlet of the tank; h_t is the heat loss coefficient at the outside surface of the tank.

2.3.3. Efficiency of hydrogen production

To initiate electrolysis of water, DC current is applied to two electrodes separated by the electrolyte. Water decomposes into hydrogen at the cathode and oxygen at the anode. Most of the commercially available electrolyzers are alkaline, using concentrated KOH as the electrolyte [15]. The half reactions taking place on the cathode and the anode in alkaline are given by

$$\text{Cathode (reduction)} : 2H_2O\ (l) + 2e^- \rightarrow H_2\ (g) + 2OH^-\ (aq) \quad (16)$$

$$\text{Anode (oxidation)} : 2OH^-\ (aq) \rightarrow 1/2O_2\ (g) + H_2O\ (l) + 2e^- \quad (17)$$

The overall water splitting reaction via electrolysis is given by

$$H_2O(aq) \rightarrow 1/2O_2\ (g) + H_2(g) \quad (18)$$

At standard conditions (25 °C and 1 bar), the splitting of water is a non-spontaneous reaction. The amount of work required to split water under these conditions equals the Gibbs free energy, ΔG° = 237 kJ/mol. In general, the minimum amount of work required can be obtained using

$$U_{rev} = \frac{\Delta G}{z * F} \tag{19}$$

where z is the number of electrons transferred per hydrogen molecule (here $z = 2$) and F is Faraday's constant (96,485 C/mol) [24].

Water decomposition is an endothermic reaction where the total amount of energy needed for water electrolysis is equivalent to the change in enthalpy ($\Delta H^\circ = 286$ kJ/mol). The remaining energy to achieve ΔH° can be supplied via heat ($T\Delta S^\circ = \Delta H^\circ - \Delta G^\circ$). Therefore the total energy demand can be expressed by the thermo-neutral cell voltage as below:

$$U_{th} = \frac{\Delta H}{z * F} \tag{20}$$

Total energy demand for both U_{rev} and U_{th} change slightly with temperature. At standard conditions (25 °C and 1 bar) $U_{rev} = 1.229$ V and $U_{th} = 1.482$ V whereas at 80 °C $U_{rev} = 1.184$ V and $U_{th} = 1.473$ V [24].

The overall efficiency of water electrolysis can be calculated using the following equation [15]:

$$\eta_{electrolysis} = \frac{U^o_{rev}}{U_{cell}} = \frac{1.23\ \text{V}}{U_{cell}} \tag{21}$$

As the typical electric potential in alkaline electrolyzers is higher than the thermoneutral voltage, water electrolysis is accompanied by the release of heat. The rate of heat produced is given by the following equation [24]:

$$\dot{Q}_{gen} = I * (U_{cell} - U_{th}) \tag{22}$$

The anodic and cathodic overpotentials are affected by the temperature of the electrodes and the electrolyzer. As the operating temperature increases for a given current density, the overpotentials decrease due to improved reaction kinetics at the electrodes [25,26]. The commercial electrolyzer operates at the voltage of 1.8–2.0 V and increasing the temperatures enables to improve the current for hydrogen production. Within this voltage range the efficiency of the electrolyzer varies between 70% and 60% [15]. Hence advanced commercial water electrolyzers use external heating to achieve operation at higher temperature [27]. Instead of external heating, we use the heat generated by the PV module to enable operation of the electrolyzer at elevated temperature. In our simulations, we used empirical electrochemical data, and temperature–potential relationships for a current flux of 25 mA/cm^2 [27], so that 100 unit electrolyzers will produce ~1 L/h of H_2 gas at standard temperature and pressure (STP). So we use the potential to be used in the calculation of the electrolysis efficiency (Eq. (21)) at this same current density of 25 mA/cm^2 for the appropriate temperature from the data in the work by Ulleberg [27]. In this prior effort, the experiments were performed with a 30% KOH solution, a nickel oxide (NiO) diaphragm, anodes based upon nickel, cobalt, and iron (Ni, Co, Fe), and a cathode based on nickel with a platinum–activated carbon catalyst (Ni, C–Pt) [27].

3. Results and discussion

3.1. COMSOL simulation and temperature distribution

We first estimated the change in the temperature throughout the PV module and the electrolyzer using FEA simulations. The velocity of the fluid, as expected, has a significant influence on the temperature distribution within these structures. Fig. S1 (see supplementary information) shows the steady state temperature distributions in a 0.4 mm thick electrolyzer chamber operated at two values of the electrolyte velocity within the chamber, 0.17 mm/s and 0.68 mm/s (75.6 μL/min and 302.4 μL/min), while the PV cell is at an ambient temperature of 25 °C and being irradiated at 1000 W/m^2. For a velocity of 0.17 mm/s, a highest temperature of 54.8 °C is reached at the top of the PV cell (top surface of the module) while the temperature at the bottom of the module is approximately 45 °C. The temperature of the electrolyte at the inlet and at the outlet was 25 °C and 52 °C, respectively. The average temperature of the electrolyte in the chamber was 53 °C. For a velocity of 0.68 mm/s, the temperature of the glass layer, the electrolyte in the chamber, and electrolyte at the outlet were 43 °C, 42 °C and 41.5 °C, respectively. So, these simulations indicate that the average electrolyte temperature is 11 °C lower (42 °C vs. 53 °C) when using the higher electrolyte velocity due to the lower residence time of the electrolyte in the electrolyzer.

Higher velocities of the coolant (electrolyte) lead to higher waste heat recovery and allow the PV cells to operate at lower temperatures and consequently higher electrical efficiency. On the other hand, a lower electrolyte temperature slows down the electrolysis reaction, resulting in lower hydrogen production efficiency. The simulations reported in the next section seek to identify conditions (electrolyte velocity, chamber thickness), that lead to an optimal temperature distribution which in turn maximizes the overall system efficiency.

3.2. Optimization of chamber thickness and electrolyzer velocity

The overall PVTE efficiency (electrical, thermal and hydrogen production) depends on the solar radiation, ambient temperature, chamber thickness, and velocity in the chamber. The first two parameters depend on the geographical location, time of the day, date, and atmospheric conditions (*e.g.*, weather), and are challenging to control. The last two parameters can be controlled through design and operation of the PVT system, and their effects have been investigated previously [9,28]. As expected, an increase in coolant velocity improves the thermal recovery from the solar cell and reduces the temperature difference between the inlet and the outlet. Similarly, a configuration with a larger coolant channel diameter but operated at the same linear flow velocity (so higher volumetric flow velocity) allows more heat to be stored in the fluid; however, the amount of useful work decreases.

In our optimization process, our objective was to maximize the overall efficiency and our constraint was to ensure that the difference in the electrolyte temperature between the inlet and the outlet exceeds 15 °C, a temperature difference needed to achieve the desired doubling in the rate of hydrogen production, as is evident from prior work by Ulleberg: an increase from 25 °C to 40 °C doubles the rate of hydrogen production at a constant voltage [27]. Furthermore, connecting the data shown in Fig. 3a and b indicates that we also should not use a temperature difference larger than 15 °C: Any larger temperature difference for any given channel diameter rapidly reduces the efficiency to a value (well) below 40%. Fig. S2 (see supplementary information) shows the flowchart for this optimization indicating the equations used, the variables, and the fixed parameters.

To evaluate the overall efficiency of the system, we considered the efficiency of the PVT and the electrolysis process described by the equation below:

$$\eta_{PVTE} = \eta_{PVT} * \eta_{electrolysis} \tag{23}$$

We performed the simulation on the entire system for different chamber thicknesses and fluid velocities under standard test conditions (irradiance of 1000 W/m^2 and 25 °C) to estimate the optimum parameters. We varied the thickness of the chamber from 1.0 mm to 0.2 mm in our simulations, guided by prior work on PEM water electrolyzers, which often have 1 mm high channels

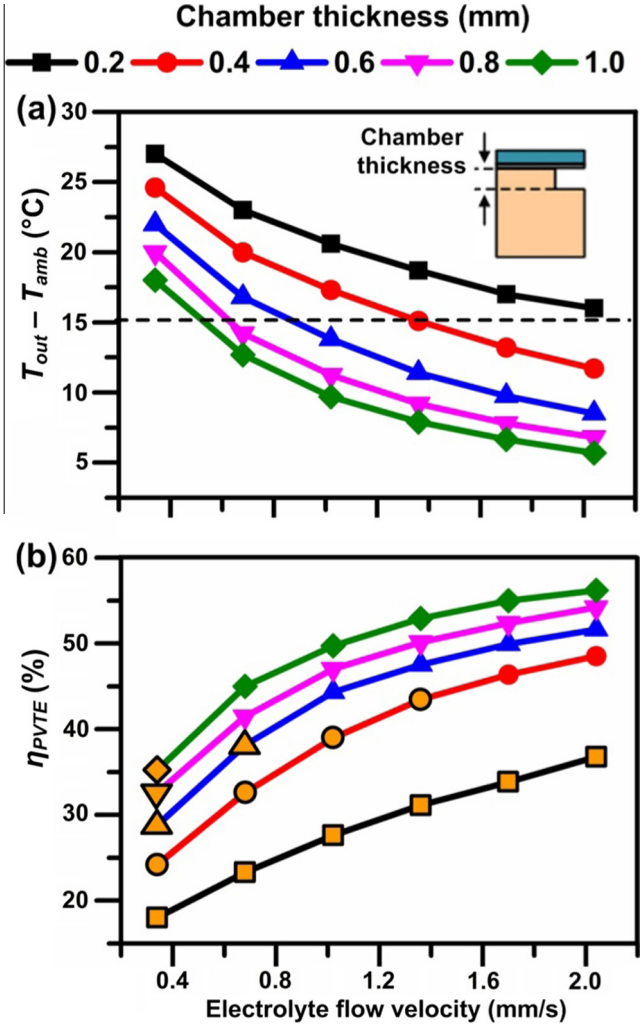

Fig. 3. Optimization of the thickness of the electrolyzer chamber and the electrolyzer flow velocity under standard test conditions for radiation (1000 W/m^2) and ambient temperature (25 °C). (a) Temperature difference between the inlet (ambient) and outlet (T_{out}) of the electrolyte as a function of flow velocity for different chamber thicknesses (indicated in inset). (b) Overall PVTE efficiency (η_{PVTE}) as a function of flow velocity for different chamber thicknesses. The data points in orange with black outlines indicate those parameters that result in the temperature difference being greater than 15 °C (above the dashed line in Fig. 3(a)).

to allow for higher rates of gas removal and bubble management in stacks of the cells [29,30]. The linear flow velocity values in the chamber were varied between ~0.3 mm/s and ~2.0 mm/s.

Fig. 3(a) shows the temperature difference between the inlet and the outlet of the electrolyte ($T_{out} - T_{amb}$), as a function of electrolyte flow velocity for different chamber thickness. The temperature difference decreases (i) with increasing flow rate due to the lower residence time, and (ii) with increasing chamber thickness due to the higher heat capacity of the fluid. A maximum temperature difference of 27 °C was observed for a velocity of 0.34 mm/s when using a 0.2 mm thick chamber. An increase of 15 °C in the temperature of the fluid between the inlet and outlet at the radiation of 1000 W/m^2 provides a thermal efficiency between 40% and 50%, which is in the range of thermal efficiency for PVT systems [31]. On the other hand, this temperature increment leads to double the rate of hydrogen production at a constant voltage [27]. Thus the data points above the dashed line in Fig. 3(a) satisfy our first objective of the optimization process. Note that using a higher electrolyte velocity or taller chambers will lead to higher overall efficiency (Fig. 3(b)), but lower hydrogen production due to a smaller temperature difference between the inlet and the outlet. As the aim of the proposed PVTE system is to maximize both overall efficiency (so it becomes comparable to those of PVT systems) and hydrogen production, we applied a design constraint on the minimum allowable temperature difference.

Fig. 3(b) shows the overall efficiency (η_{PVTE}) as a function of the electrolyte flow velocity for different values of chamber thickness. The overall efficiency increases significantly upon increasing the electrolyte velocity and/or the chamber thickness. Higher electrolyte flow velocities lead to better heat removal, hence a lower operation temperature of the PV module, thus enhancing its efficiency. This effect seems to dominate over the increase in the efficiency of the electrolysis process when operating at lower flow velocities (resulting in a higher electrolyte temperature and thus better kinetics in the electrolyzer). Similarly, an increase in chamber thickness enhances the capacity for heat removal (higher volumetric flow rate of electrolyte), which in turn leads to a lower temperature of the PV module.

The data points above the dashed line in Fig. 3(a) are marked with orange with black outlines in Fig. 3(b); these data points correspond to the parameter values for which the temperature difference exceeds 15 °C. Constrained by the condition of a minimum temperature difference of 15 °C, a maximum overall efficiency of 43% can be achieved when using a chamber thickness of 0.4 mm and operating at an electrolyte velocity of 1.36 mm/s. Naturally, different values of solar radiation and ambient temperature may lead to different optimum values for these parameters, yet the observed trends are expected to remain the same. In the following sections, we will use the identified optimum values of the chamber thickness (0.4 mm) and fluid velocity (1.36 mm/s) to estimate the hourly and annually efficiency of the PVTE system.

3.3. Hourly variations of PVTE efficiency

To evaluate the practical feasibility of the PVTE system, we examined the hourly performance of the PVTE system using solar radiation and temperature data from Phoenix, AR in May 2010 [32]. This data was chosen because this location is designated as Class I by the U.S. Department of Energy's (DOE) National Renewable Energy Laboratory (NREL), meaning that the solar radiation and temperature values are complete and highly accurate [32]. We used the optimized values for the chamber thickness and the velocity, 0.4 mm and 1.36 mm/s, respectively. Fig. 4(a) represents the average hourly radiation and ambient temperature data, along with the simulated temperatures of the PV cell in the presence and absence of the electrolyzer. As expected the temperatures of the PV cell within the PVTE and the stand-alone PV cell peaked at noon, at temperatures of 65.3 °C and 48.7 °C respectively. More importantly, addition of the electrolyzer reduced the temperature of the PV system with the maximum reduction (~17 °C decrease) occurring at noon [6,33]. The electrical efficiencies of these PV cells are shown in Fig. 4(b). The PV cell embedded in PVTE performed better than the stand-alone PV cell due to the active cooling of the PV cells by electrolyzer. The improvement in the electrical efficiency was most significant at noon time. Fig. 4(b) also shows (right vertical axis) the gain in electrical power output when the PVTE module is used instead of the stand-alone PV module. For monocrystalline and polycrystalline cells, the electrical power output efficiency decreases by 0.5% per °C temperature increase [34]. Hence, a reduction of ~17 °C of the PVTE compared to the stand-alone PV module led to an improvement of ~8% in power output efficiency.

The overall PVTE efficiencies calculated based on 1st (Eq. (13)) and 2nd (Eq. (14)) law are shown in Fig. 4(c). As explained before, the 1st law represents the heat gain from the system whereas the 2nd law indicates the work potential. Although the amount of heat recovery increased for the solar cell at noon, the energetic PVTE effi-

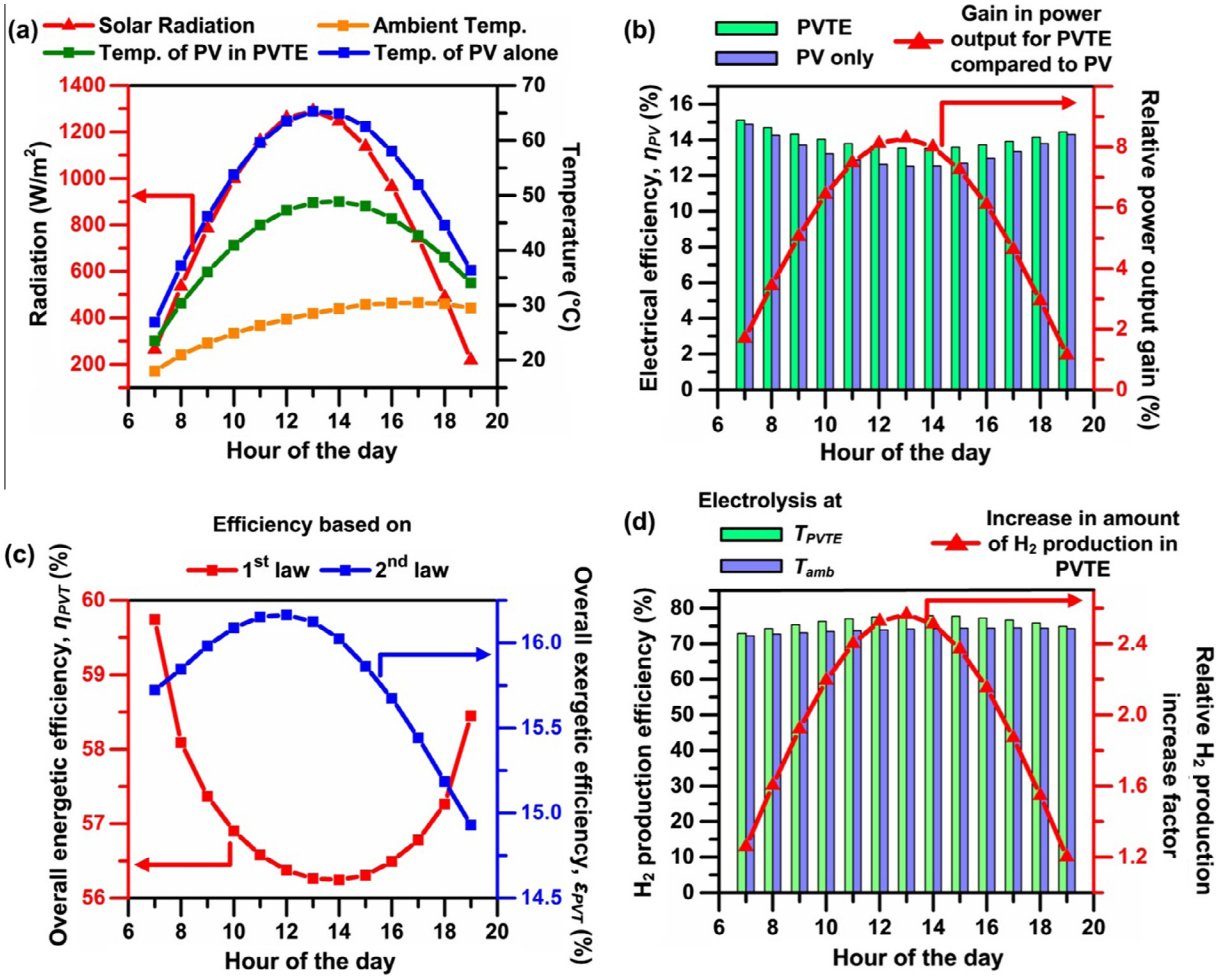

Fig. 4. Hourly variations in temperatures of the PV modules and the various efficiencies based on actual data from May 21, 2010 for Phoenix, AR [32]. (a) Average hourly radiation and ambient temperature data in May, along with the temperatures of the PV module integrated within the PVTE system and a stand-alone PV module. (b) Average hourly variations in the electrical efficiency of the PV module for the PVTE and the stand-alone PV panel. The relative power output gain (right axis) represents the percentage increase in the efficiency by using the PVTE system instead of the stand-alone PV. (c) Average hourly variations in overall energetic (1st law, left axis) and exergetic (2nd law, right axis) efficiencies of the PVTE systems (sum of electrical and thermal). (d) Average hourly variations in H_2 production efficiency of the electrolyzer of the PVTE system and of the electrolyzer operating at ambient temperatures. The relative increase factor (right axis) represents the increase in the amount of H_2 production of the PVTE operating at a higher temperature instead of an electrolyzer operating at ambient temperature.

ciency decreased from 60% to 56% due to heat loss from the system. Of this 4% drop in efficiency, 2.5% resulted from a decrease in waste heat recovery and 1.5% from a decrease in electrical efficiency. On the other hand, the exergetic PVTE efficiency peaked at noon even as the electrical efficiency decreased, because the work potential increased. The temperature difference between the inlet and outlet of the electrolyzer is the key parameter for exergetic thermal efficiency, and peaks at ~17 °C at noon, evident from Fig. 4(a).

Fig. 4(d) compares the hydrogen production efficiency at the actual temperature in the PVTE module (see Fig. 4(a)) and at ambient temperature, as a function of the hour of the day. Again, as expected, the hydrogen production efficiency peaked at noon because the temperature of the PV module (~48 °C) and consequently of the electrolyzer was highest at that time. Furthermore, the higher operating temperatures of the electrolyzer within the PVTE module led to a higher efficiency of hydrogen production compared to the efficiency of the same electrolyzer operating at ambient temperature. The increase in hydrogen production efficiency peaked at noon time, 78% for the electrolyzer within the PVTE compared to 74% for the electrolyzer at ambient temperature. The right vertical axis of Fig. 4(d) shows the extent by which the hydrogen production increases when operating the electrolyzer within the PVTE (and thus at higher temperature) as opposed to electrolyzer at ambient temperature. When the hydrogen production rate was 25 mA/cm^2, the efficiency was 74% when the electrolyzer operated at ambient temperature of 28 °C. Within the PVTE, the waste heat from the PV module resulted in an increase in the electrolyzer temperature to ~48 °C, which led to increase in the hydrogen production rate to 60 mA/cm^2 for the same applied potential [27], an almost 2.5-fold increase in hydrogen production.

3.4. Monthly variations of PVTE efficiency

Similar to the hourly analysis in the previous sub-section, we examined the monthly variations in the electrical, thermal, and hydrogen production efficiencies using the climate data for Phoenix, AZ from 2010 [32]. All data shown in Fig. 5 represent the average values for the efficiencies for each month. Fig. 5(a) indicates that the electrical efficiency and the power output of the PV module within the PVTE system were higher than the corresponding values for a stand-alone PV because of the enhanced waste heat removal in the PVTE system. The electrical efficiency decreased during summer months due to the higher ambient temperatures causing an increase in the temperature of the PV module. In certain

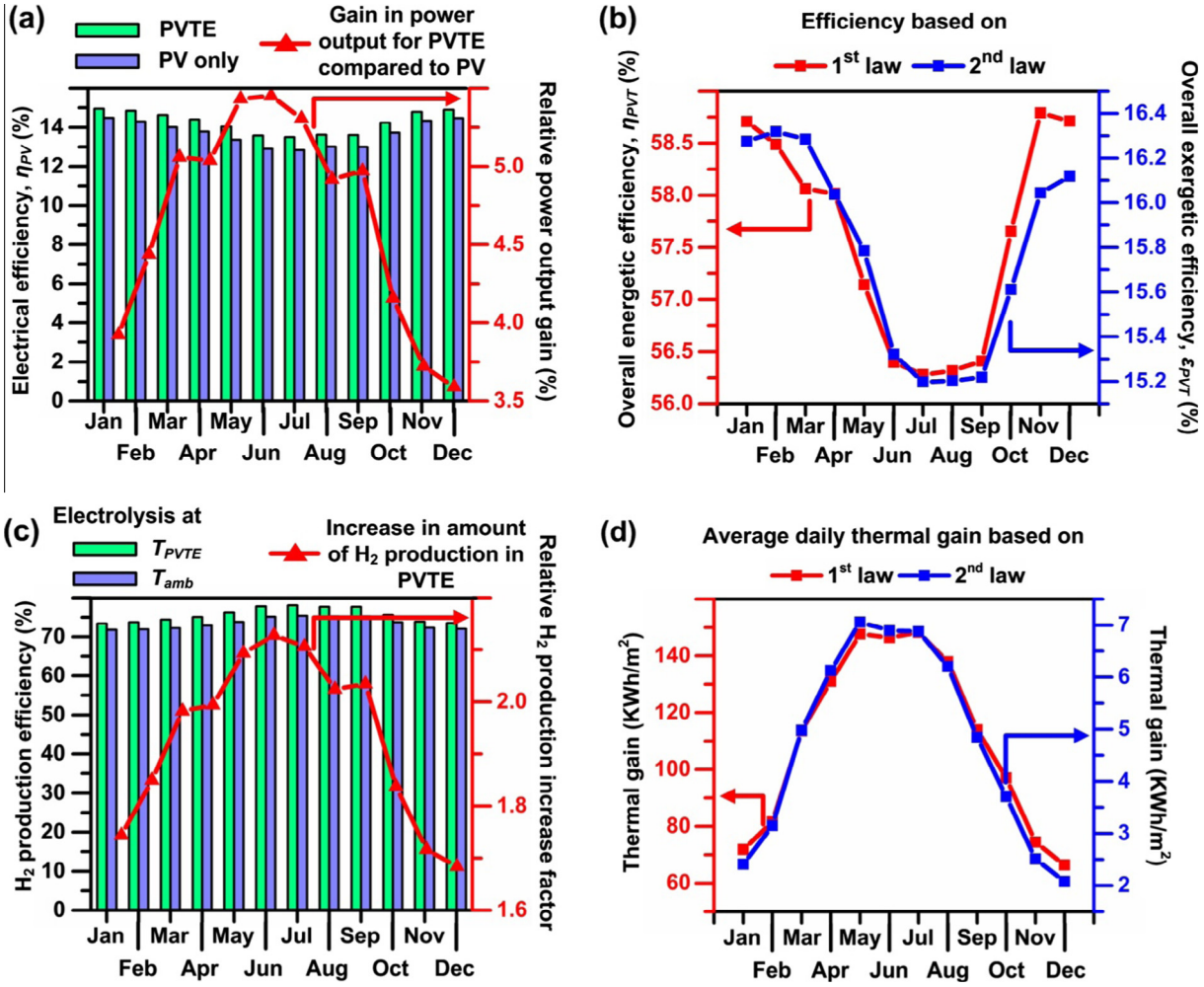

Fig. 5. Monthly variations in the different efficiencies based on data for Phoenix, AR in 2010. (a) Average monthly variations in the electrical efficiency of the PV module for the PVTE and the stand-alone PV panel. The relative power output gain (right axis) represents the percentage increase in the efficiency by using the PVTE system instead of the stand-alone PV. (b) Average monthly variations in overall energetic (1st law, left axis) and exergetic (2nd law, right axis) efficiencies of the PVTE systems (sum of electrical and thermal). (c) Average monthly variations in H_2 production efficiency of the PVTE system and of the electrolyzer operating at ambient temperatures. The relative increase factor (right axis) represents the increase in the amount of H_2 production of the PVTE operating at a higher temperature instead of an electrolyzer operating at ambient temperature. (d) Average monthly thermal gain of the PVTE system based on the 1st law (left axis) and the 2nd law (right axis).

summer months the improvement in electrical efficiency of the PVTE compared to a stand-alone PV led to an increase of more than 5% in the average power output. The gain is higher during summer because the effect of active cooling by the electrolyzer (reducing the temperature of the PV module) is more dominant when the ambient temperature is higher.

Both the energetic and exergetic efficiencies of the PVTE decreased during summer (Fig. 5(b)), mainly because the higher ambient temperature during the summer leads to a decrease in the difference between the electrolyte and ambient temperature. Although the flow rate can be increased to increase the thermal gain and reduce the operating temperature of PV cell, this increase in flow rate will decrease the efficiency of the electrolysis process and the exergetic efficiency, which in turn will adversely affect the overall efficiency of the system. The energetic and exergetic energy values for the thermal gain increased during summer months (Fig. 5(d)), even though the energetic and exergetic PVTE efficiencies decreased. Overall, the energetic efficiencies of the PVTE system varied between 56% and 59% during the year, which is comparable to the values reported previously for PVT systems (52–58%) [12].

We also estimated the monthly variations in the hydrogen production efficiency and the factor by which it increases as a function of operation temperature (Fig. 5(c)). The analysis results show that the higher solar radiation and higher ambient temperature in the summer months has a positive effect on the efficiency of hydrogen production, with the highest efficiency value obtained in the month of July for both the integrated PVTE system and the electrolyzer alone when operating at ambient temperature. The gain in efficiency of H_2 production in the PVTE system compared to that in an electrolyzer at ambient temperatures was higher from June to September as a result of higher electrolyte temperatures in the PVTE system. More importantly, this analysis shows that the amount of H_2 produced in the PVTE system was at least 2-fold higher for seven months of the year compared to the amount of H_2 produced in the electrolyzer alone, when operating at ambient temperatures.

4. Conclusion

This paper reported an energetic analysis of a photovoltaic system that integrates a photovoltaic (PV) module with an electrolyzer, referred to as a photovoltaic thermal water electrolyzer

(PVTE). Active cooling of the PV module by the electrolyte in the electrolyzer reduces the temperature of the PV module and consequently increases the electrical efficiency. The heat absorbed by the electrolyte enhances the reaction kinetics of the electrolysis process leading to more efficient production of hydrogen.

We used FEA simulations to optimize the geometry (specifically electrolyzer dimensions) and operating conditions (specifically electrolyte flow rate) to maximize the overall energy efficiency of the PVTE system and the amount of hydrogen produced. Then we used the optimized geometry and operating conditions to perform a comprehensive energy analysis (daily and annually) using solar radiation and ambient temperature data from Phoenix, Arizona. The improvement in power output gain of the PVTE system compared to a stand-alone PV module was highest during afternoon and during summer months, when the ambient temperatures are the highest. Similarly, the increase in the amount of hydrogen production of the PVTE system compared to an electrolyzer operating at ambient temperature was highest during afternoon and during summer months.

Overall the use of PVTE system to generate hydrogen provides a more useful, versatile and efficient way to utilize the removed waste heat compared to current PVT systems. In addition to the water and/or room heating, the produced hydrogen can be used for other energy applications, such as powering fuel cell-based cars. The inclusion of additional elements for electrolysis (electrodes, voltage source, etc.) in the PVTE system will increase the complexity and cost compared to current PVT system. The added benefit of hydrogen production, however, is expected to compensate for the increased cost and complexity [35,36].

In the current analysis, we assumed a constant flow rate of the electrolyzer. The flow rate, however, can be regulated based on active feedback from a thermometer and pyrheliometer that measure the temperature of the PVTE system and the solar radiation value, respectively. As flow rate determines the time scale of heat transfer and consequently the temperatures at various locations of the PVTE system, active feedback control of the flow rate will enable control over the individual output efficiencies depending on time of the day and/or year, *e.g.*, higher thermal output during winter or higher electrolysis output during summer.

Acknowledgements

We acknowledge support for this work (MEO and RGN) as part of the 'Light-Material Interactions in Energy Conversion' Energy Frontier Research Center funded by the U.S. Department of Energy, Office of Basic Energy Sciences under Award Number DE-SC0001293. We also acknowledge financial support from the National Science Foundation under awards CMMI 03-28162 and CMMI 07-49028 to Nano-CEMMS, a Nano Science & Engineering Center (NSEC) on Nanomanufacturing, for PJAK and AVD.

Appendix A. Supplementary material

Supplementary data associated with this article can be found, in the online version, at http://dx.doi.org/10.1016/j.apenergy.2015.11.078.

References

[1] Global market outlook for photovoltaics until 2016. European Photovoltaic Industry Association, EPIA; 2012.
[2] Parida B, Iniyan S, Goic R. A review of solar photovoltaic technologies. Renew Sustain Energy Rev 2011;15:1625–36.
[3] Peter LM. Towards sustainable photovoltaics: the search for new materials. Philos Trans Roy Soc A – Math Phys Eng Sci 2011;369:1840–56.
[4] Yoon J, Li LF, Semichaevsky AV, Ryu JH, Johnson HT, Nuzzo RG, et al. Flexible concentrator photovoltaics based on microscale silicon solar cells embedded in luminescent waveguides. Nat Commun 2011;2:1–8 343.
[5] Karam NH, King RR, Haddad M, Ermer JH, Yoon H, Cotal HL, et al. Recent developments in high-efficiency $Ga_{0.5}In_{0.5}P$/GaAs/Ge dual- and triple-junction solar cells: steps to next-generation PV cells. Sol Energy Mater Sol Cells 2001;66:453–66.
[6] Tiwari GN, Mishra RK, Solanki SC. Photovoltaic modules and their applications: a review on thermal modelling. Appl Energy 2011;88:2287–304.
[7] Skoplaki E, Palyvos JA. On the temperature dependence of photovoltaic module electrical performance: a review of efficiency/power correlations. Sol Energy 2009;83:614–24.
[8] Royne A, Dey CJ, Mills DR. Cooling of photovoltaic cells under concentrated illumination: a critical review. Sol Energy Mater Sol Cells 2005;86:451–83.
[9] Charalambous PG, Maidment GG, Kalogirou SA, Yiakoumetti K. Photovoltaic thermal (PV/T) collectors: a review. Appl Therm Eng 2007;27:275–86.
[10] Shah A, Torres P, Tscharner R, Wyrsch N, Keppner H. Photovoltaic technology: the case for thin-film solar cells. Science 1999;285:692–8.
[11] Kalogirou SA. Solar thermal collectors and applications. Prog Energy Combust Sci 2004;30:231–95.
[12] Chow TT. A review on photovoltaic/thermal hybrid solar technology. Appl Energy 2010;87:365–79.
[13] Pathak MJM, Sanders PG, Pearce JM. Optimizing limited solar roof access by exergy analysis of solar thermal, photovoltaic, and hybrid photovoltaic thermal systems. Appl Energy 2014;120:115–24.
[14] Nowotny J, Veziroglu TN. Impact of hydrogen on the environment. Int J Hydrogen Energy 2011;36:13218–24.
[15] Zeng K, Zhang DK. Recent progress in alkaline water electrolysis for hydrogen production and applications. Prog Energy Combust Sci 2010;36:307–26.
[16] Jones AD, Underwood CP. A thermal model for photovoltaic systems. Sol Energy 2001;70:349–59.
[17] Yang DJ, Yuan ZF, Lee PN, Yin HM. Simulation and experimental validation of heat transfer in a novel hybrid solar panel. Int J Heat Mass Transf 2012;55:1076–82.
[18] Santbergen R. Optical absorption factor of solar cells for PVT systems [dissertation]. Eindhoven University; 2008.
[19] Fujisawa T, Tani T. Annual exergy evaluation on photovoltaic-thermal hybrid collector. Sol Energy Mater Sol Cells 1997;47:135–48.
[20] Evans DL, Florschuetz LW. Cost studies on terrestrial photovoltaic power-systems with sunlight concentration. Sol Energy 1977;19:255–62.
[21] Chow TT. Performance analysis of photovoltaic-thermal collector by explicit dynamic model. Sol Energy 2003;75:143–52.
[22] Bhargava AK, Garg HP, Agarwal RK. Study of a hybrid solar-system solar air heater combined with solar-cells. Energy Convers Manage 1991;31:471–9.
[23] Chow TT, Pei G, Fong KF, Lin Z, Chan ALS, Ji J. Energy and exergy analysis of photovoltaic-thermal collector with and without glass cover. Appl Energy 2009;86:310–6.
[24] Dieguez PM, Ursua A, Sanchis P, Sopena C, Guelbenzu E, Gandia LM. Thermal performance of a commercial alkaline water electrolyzer: experimental study and mathematical modeling. Int J Hydrogen Energy 2008;33:7338–54.
[25] Appleby AJ, Crepy G, Jacquelin J. High-efficiency water electrolysis in alkaline-solution. Int J Hydrogen Energy 1978;3:21–37.
[26] Hug W, Divisek J, Mergel J, Seeger W, Steeb H. Highly efficient advanced alkaline electrolyzer for solar operation. Int J Hydrogen Energy 1992;17:699–705.
[27] Ulleberg O. Modeling of advanced alkaline electrolyzers: a system simulation approach. Int J Hydrogen Energy 2003;28:21–33.
[28] Teo HG, Lee PS, Hawlader MNA. An active cooling system for photovoltaic modules. Appl Energy 2012;90:309–15.
[29] Casati C, Longhi P, Zanderighi L, Bianchi F. Some fundamental aspects in electrochemical hydrogen purification/compression. J Power Sources 2008;180:103–13.
[30] Grigoriev SA, Kalinnikov AA, Millet P, Porembsky VI, Fateev VN. Mathematical modeling of high-pressure PEM water electrolysis. J Appl Electrochem 2010;40:921–32.
[31] Tripanagnostopoulos Y, Nousia T, Souliotis M, Yianoulis P. Hybrid photovoltaic/thermal solar systems. Sol Energy 2002;72:217–34.
[32] NREL. National solar radiation data base: 1991–2010 update: data for phoenix, AR on May 21. <http://rredc.nrel.gov/solar/old_data/nsrdb/1991-2010/hourly/list_by_state.html>; 2010 [retrieved on October 10, 2015].
[33] Rajoria CS, Agrawal S, Tiwari GN. Exergetic and enviroeconomic analysis of novel hybrid PVT array. Sol Energy 2013;88:110–9.
[34] Mattei M, Notton G, Cristofari C, Muselli M, Poggi P. Calculation of the polycrystalline PV module temperature using a simple method of energy balance. Renewable Energy 2006;31:553–67.
[35] Murphy OJ, Bockris JOM. Photovoltaic electrolysis: hydrogen and electricity from water and light. Int J Hydrogen Energy 1984;9:557–61.
[36] Rodriguez CA, Modestino MA, Psaltis D, Moser C. Design and cost considerations for practical solar-hydrogen generators. Energy Environ Sci 2014;7:3828–35.